

Qatar Exoplanet Survey : Qatar-3b, Qatar-4b and Qatar-5b.

Khalid A. Alsubai^{1*}, Dimitris Mislis¹, Zlatan I. Tsvetanov¹, David W. Latham², Allyson Bieryla², Lars A. Buchhave³, Gilbert A. Esquerdo², D.M. Bramich¹, Stylianos Pyrzas¹, Nicolas P. E. Vilchez¹, Luigi Mancini^{4, 5}, John Southworth⁶, Daniel F. Evans⁶, Thomas Henning⁷, Simona Ciceri⁴

¹Qatar Environment and Energy Research Institute (QEERI), HBKU, Qatar Foundation, PO Box 5825, Doha, Qatar

²Harvard-Smithsonian Center for Astrophysics, 60 Garden Street, Cambridge, MA 02138, USA

³Centre for Star and Planet Formation, Natural History Museum of Denmark & Niels Bohr Institute, University of Copenhagen, Øster Voldgade 5-7, DK-1350 Copenhagen K, Denmark

⁴Max Planck Institute for Astronomy, Königstuhl 17, D-69117 Heidelberg, Germany

⁵INAF-Osservatorio Astrofisico di Torino, via Osservatorio 20, 10025, Pino Torinese, Italy

⁶Astrophysics Group, Keele University, Staffordshire ST5 5BG, UK

⁷Department of Astronomy, Stockholm University, AlbaNova University Centre, SE-106 91 Stockholm, Sweden

Accepted . Received 1;

ABSTRACT

We report the discovery of Qatar-3b, Qatar-4b, and Qatar-5b, three new transiting planets identified by the Qatar Exoplanet Survey (QES). The three planets belong to the hot Jupiter family, with orbital periods of $P_{Q3b} = 2.5079204$ days, $P_{Q4b} = 1.8053949$ days, and $P_{Q5b} = 2.8792319$ days. Follow-up spectroscopic observations reveal the masses of the planets to be $M_{Q3b} = 4.31 M_J$, $M_{Q4b} = 5.85 M_J$, and $M_{Q5b} = 4.32 M_J$, while model fits to the transit light curves yield radii of $R_{Q3b} = 1.096 R_J$, $R_{Q4b} = 1.552 R_J$, and $R_{Q5b} = 1.107 R_J$. No evidence of eccentric orbit is seen in the radial velocity curve of any of the planets. The host stars are typical main sequence stars with masses and radii $M_{Q3} = 1.145 M_\odot$, $M_{Q4} = 0.954 M_\odot$, $M_{Q5} = 1.128 M_\odot$ and $R_{Q3} = 1.272 R_\odot$, $R_{Q4} = 1.115 R_\odot$ and $R_{Q5} = 1.076 R_\odot$ for the Qatar-3, 4 and 5 respectively. All three new planets can be classified as heavy hot Jupiters ($M > 4 M_J$), while Qatar-5 is among the most metal-rich stars known to host a planet.

Key words: techniques: photometric - planets and satellites: detection - planets and satellites: fundamental parameters - planetary systems.

1 INTRODUCTION

Ground-based surveys for transiting exoplanets continue to be a productive source for finding short period giant planets orbiting relatively bright stars. Many of these discoveries have become primary targets for subsequent studies of exoplanetary atmospheres and other important planetary characteristics with the use of some of the most advanced ground- and space-based telescopes. In addition, these discoveries contribute significantly to a more complete census of hot Jupiters and other close orbiting large planets – the type of planets not present in our solar system – and may provide a key to understanding their origin and more generally the planetary system architecture.

This paper is based on observations collected with the first generation of the Qatar Exoplanet Survey (QES, Alsubai et al. 2013). QES uses two overlapping wide field 135mm (f/2.0) and 200mm

(f/2.0) telephoto lenses, along with four 400mm (f/2.8) telephoto lenses, mosaiced to image an $11^\circ \times 11^\circ$ field on the sky simultaneously at three different pixel scales. With its larger aperture lenses and its higher angular resolution (a result of the longer focal length of the lenses), QES is able to go 0.5 mag deeper than other ground-based, wide-angle survey systems, such as SuperWASP (Pollaco et al. 2006), HATNet (Bakos et al. 2004) and TrES (Alonso et al. 2004).

The paper is organized as follows: in section 2 we present the survey photometry and describe the follow-up spectroscopy and photometry used to confirm the planetary nature of the transits. In section 3 we present the global system solutions using simultaneous fit to the available RV and follow-up photometric light curves with the stellar parameters determined from the combined spectra, while in Section 4 we summarise our results.

* E-mail: kalsubai@qf.org.qa

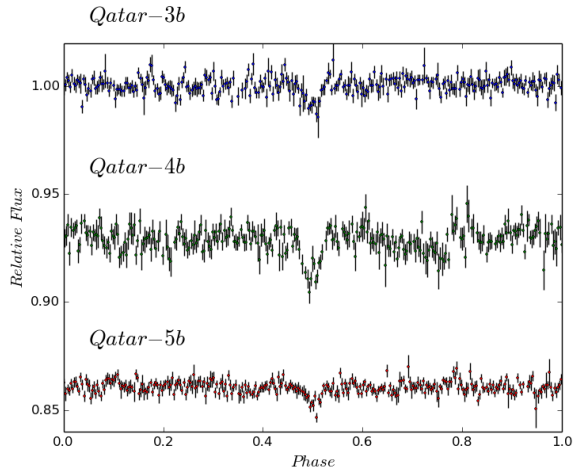


Figure 1. The discovery light curves phase folded with the BLS estimated periods, as they appear in the QES archive, for Qatar-3b (top, in blue), Qatar-4b (middle, in green), and Qatar-5b (bottom, in red) [color available in the on-line version only]. For clarity, all light curves have been binned, while those of Qatar-4b and Qatar-5b have been shifted downwards.

2 OBSERVATIONS

2.1 Discovery photometry

Observations for the discovery photometry were collected at the QES station in New Mexico, USA. QES utilizes FLI ProLine PL6801 cameras, with KAF-1680E 4k×4k detectors. Exposure times were 60s, for each of the four CCDs attached to the 400mm lenses; 45s, for the CCD equipped with the 200mm lens; and 30s, for the CCD equipped with the 135mm lens.

The survey data were reduced with the QES-pipeline, which performs bias-correction, dark-current subtraction and flat-fielding in the standard fashion, while photometric measurements are extracted using the image subtraction algorithm by Bramich (2008); a more detailed description of the pipeline is given in Alsubai et al. (2013).

The output light curves were ingested into the QES archive and subsequently subjected to a combination of the Trend Filtering Algorithm (TFA, Kovács et al. 2005) and the SysRem algorithm (Tamuz et al. 2005), to model and remove systematic patterns of correlated noise. Transit-like events for all three stars were revealed during a search on the archive light curves using the Box Least Square algorithm (BLS) of Kovács et al. (2002). The BLS algorithm provided tentative ephemerides which were used to phase-fold the discovery light curves shown in Figure 1.

The discovery light curve of Qatar-3b contains data points from 11,228 frames, spanning a period from October 2012 to January 2015, that of Qatar-4b contains data points from 8,950 frames, with a time-span from September 2012 to November 2014, and that of Qatar-5b contains 18,957 data points, with a time-span from September 2012 to December 2014.

2.2 The host stars

Qatar-3b’s host is a $V = 12.88$ mag ($B = 13.13$ mag) star of spectral type very close to G0V. The host of Qatar-4b is a $V = 13.60$ mag ($B = 14.69$ mag), early-K type star, and, similarly, the host of Qatar-5b is a $V = 12.82$ mag ($B = 13.00$ mag) star of spectral type close to G2V. The basic observational characteristics of the three host stars,

Table 1. Basic observational and spectroscopic parameters of the host stars

Parameters	Qatar-3	Qatar-4	Qatar-5
V [mag]	12.88	13.60	12.82
B [mag]	13.13	14.69	13.00
J [mag]	11.60	13.61	11.35
Spectral Types	G0V	K1V	G2V
T_{eff} [K]	6007 ± 52	5219 ± 50	5747 ± 49
$\log g$ [cgs]	4.286 ± 0.079	4.323 ± 0.023	4.427 ± 0.035
[M/H]	-0.041 ± 0.081	0.166 ± 0.081	0.377 ± 0.080
$v \sin i$ [km s^{-1}]	10.2 ± 0.5	7.1 ± 0.5	4.5 ± 0.5

together with the results from the spectroscopic analysis, are listed in Table 1. We further discuss stellar parameters determined from our follow-up spectra in section 3.1. The host star spectral types are estimated from a multi-color fit (J, H, V and K band) using the UCAC3 values.

2.3 Follow-up spectroscopy

Follow-up spectroscopic observations of all three candidates were obtained with the Tillinghast Reflector Echelle Spectrograph (TRES) on the 1.5 m Tillinghast Reflector at the Fred L. Whipple Observatory on Mount Hopkins, Arizona. Similarly to our campaigns for all QES candidates we used TRES with the medium fiber, which yields a resolving power of $R \sim 44,000$, corresponding to a velocity resolution element of 6.8 km s^{-1} FWHM. The spectra were extracted using version 2.55 of the code described in Buchhave et al. (2010). The wavelength calibration for each spectrum was established using exposures of a thorium-argon hollow-cathode lamp illuminating the science fiber, obtained immediately before and after each observation of the star.

For Qatar-3 a total of 27 spectra were obtained between 2015-07-30 (UT) and 2016-01-03 with a typical exposure time of 30 min and an average signal-to-noise ratio per resolution element (SNRe) of 29 at the peak of the continuum in the echelle order centered on the Mg b triplet near 519 nm. For Qatar-4 we obtained 8 usable spectra between 2015-09-23 and 2016-02-09 with mostly 48-min exposures and $\langle \text{SNRe} \rangle = 22$, and for Qatar-5 a total of 25 usable spectra between 2015-09-27 and 2015-12-08 with mostly 25-min exposures and $\langle \text{SNRe} \rangle = 29$.

Relative radial velocities (RV) were derived by cross-correlating each observed spectrum against the strongest exposure of the same star, order by order for a set of echelle orders selected to have good SNRe and minimal contamination by telluric lines introduced by the Earth’s atmosphere. These RVs are reported in Tables 2, 3, and 4. The observation that was used for the template spectrum for each star has, by definition, an RV of 0.00 km s^{-1} . We also derived values for the line profile bisector spans (BS), to check for astrophysical phenomena other than orbital motion that might produce a periodic signal in the RVs with the same period as the photometric ephemerides for the transits. The procedures used to determine RVs and BSs are outlined in Buchhave et al. (2010).

To illustrate the quality of the orbital solutions provided by our relative radial velocities, we fit circular orbits with the epoch and period set to the final ephemerides values from the global analysis. The key parameters for these orbital solutions are reported in Table 5, and the corresponding velocity curves and individual observations are plotted in Figures 2, 3, and 4. Note that the relative

Table 2. Relative RVs and BS variations for Qatar-3.

BJD	RV (m s^{-1})	BS (m s^{-1})
2457233.9060	1314 ± 49	266 ± 40
2457237.8276	337 ± 77	236 ± 77
2457263.8334	1464 ± 101	39 ± 38
2457271.9555	1089 ± 120	200 ± 87
2457273.8826	927 ± 51	6 ± 54
2457284.8017	732 ± 102	23 ± 79
2457285.9482	242 ± 75	-31 ± 54
2457288.7856	798 ± 58	-42 ± 39
2457289.8705	718 ± 77	-47 ± 31
2457291.6720	1042 ± 77	48 ± 31
2457292.7829	85 ± 53	-15 ± 29
2457293.7437	194 ± 64	21 ± 36
2457294.8549	228 ± 106	-7 ± 35
2457295.9123	126 ± 59	-30 ± 41
2457296.8432	956 ± 70	7 ± 38
2457297.7507	19 ± 70	-14 ± 28
2457298.8203	647 ± 62	-31 ± 21
2457299.7981	713 ± 113	28 ± 57
2457303.8631	730 ± 77	47 ± 73
2457304.8158	711 ± 96	-91 ± 57
2457315.6195	92 ± 128	-73 ± 87
2457318.6972	291 ± 60	-83 ± 45
2457328.8461	591 ± 69	-63 ± 35
2457332.8579	281 ± 64	-49 ± 72
2457351.6699	953 ± 53	-325 ± 37
2457357.6141	636 ± 75	-17 ± 29
2457390.6129	0 ± 49	2 ± 37

Table 3. Relative RVs and BS variations for Qatar-4.

BJD	RV (m s^{-1})	BS (m s^{-1})
2457288.8607	1880 ± 71	31 ± 43
2457296.8824	0 ± 50	-14 ± 37
2457297.8655	1784 ± 50	-21 ± 26
2457327.7940	-31 ± 60	53 ± 37
2457356.6018	-51 ± 51	-51 ± 33
2457390.6675	234 ± 51	-49 ± 28
2457409.6606	2200 ± 84	54 ± 42
2457417.6154	587 ± 75	-1 ± 23

gamma velocity is the center-of-mass velocity using the relative velocities.

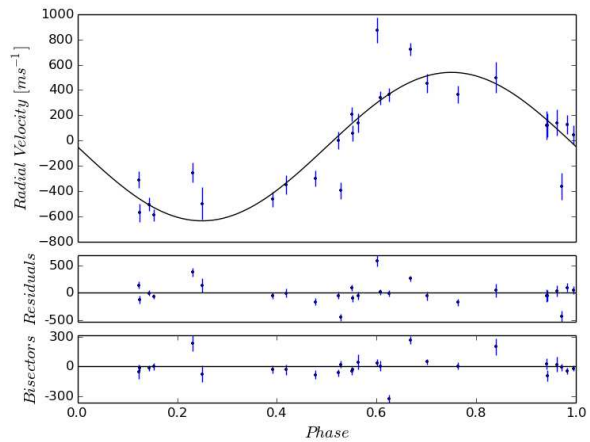
To get the absolute gamma (center-of-mass) velocity for a system where we use the multi-order relative velocities to derive the orbital solution, we have to provide an absolute velocity for the observation that was used for the template when deriving the relative velocities. By definition that observation is assigned a relative velocity of 0.00 km s^{-1} . To derive an absolute velocity for that observation, we correlate the Mg b order against the template from the CfA library of synthetic templates that gives the highest peak correlation value. Then we add the relative gamma velocity from the orbital solution, and also correct by -0.61 km s^{-1} , mostly because the CfA library does not include the gravitational redshift. This offset has been determined empirically by many observations of IAU Radial Velocity Standard Stars. We quote an uncertainty in the resulting absolute velocity of $\pm 0.1 \text{ km s}^{-1}$, which is an estimate of the residual systematic errors in the IAU Radial Velocity Standard Star system.

Table 4. Relative RVs and BS variations for Qatar-5.

BJD	RV (m s^{-1})	BS (m s^{-1})
2457292.7383	991 ± 29	160 ± 28
2457296.9362	-5 ± 31	81 ± 31
2457298.8466	950 ± 28	34 ± 17
2457299.7752	95 ± 38	-17 ± 24
2457318.7366	1050 ± 27	-9 ± 24
2457327.8283	828 ± 33	5 ± 28
2457328.6901	-92 ± 29	-3 ± 19
2457329.8154	680 ± 31	-2 ± 27
2457332.8336	823 ± 27	-12 ± 24
2457345.7245	58 ± 37	1 ± 21
2457346.6775	210 ± 27	16 ± 21
2457347.6982	984 ± 15	-3 ± 15
2457348.6916	0 ± 15	-16 ± 10
2457349.6621	260 ± 23	-38 ± 25
2457350.6435	837 ± 30	-41 ± 21
2457351.6976	-235 ± 20	-28 ± 11
2457354.6615	-186 ± 30	-33 ± 17
2457355.7121	632 ± 30	-28 ± 22
2457356.6458	811 ± 26	5 ± 15
2457357.6722	-95 ± 30	2 ± 21
2457358.7104	741 ± 25	-24 ± 21
2457360.6173	-108 ± 32	1 ± 28
2457361.6212	775 ± 28	-48 ± 19
2457362.6705	464 ± 24	5 ± 22
2457364.6030	919 ± 27	-4 ± 20

Table 5. Initial Orbital Parameters.

Orbital Parameter	Qatar-3b	Qatar-4b	Qatar-5b
Semi-amplitude K (m s^{-1})	567 ± 70	1056 ± 88	556 ± 17
Relative γ (m s^{-1})	535 ± 44	966 ± 74	421 ± 13
Absolute γ (km s^{-1})	$+6.04 \pm 0.1$	-28.76 ± 0.1	-9.54 ± 0.1
RMS RV residuals (m s^{-1})	217	207	67
Number of RVs	27	8	25


Figure 2. Orbital solution for Qatar-3b, showing the velocity curve and observed velocities.

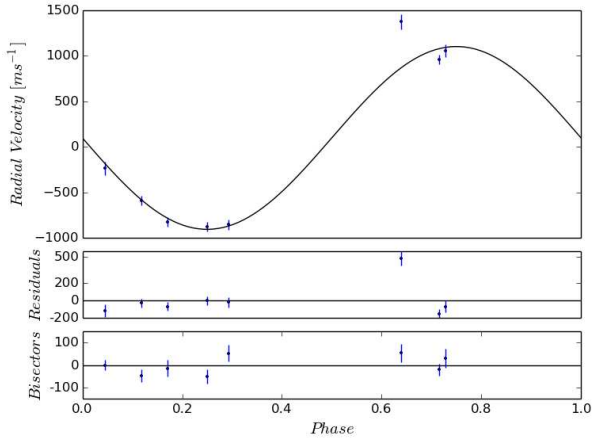


Figure 3. Orbital solution for Qatar-4b, showing the velocity curve and observed velocities.

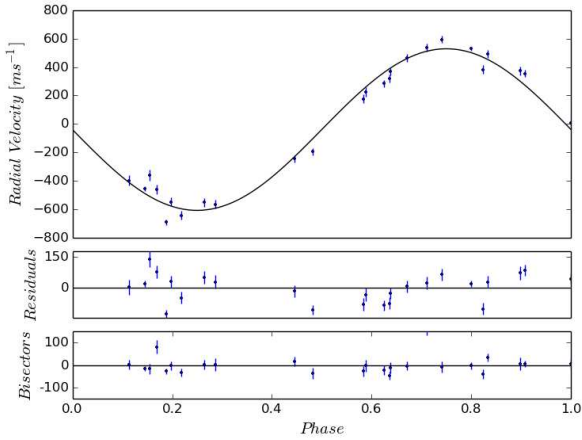


Figure 4. Orbital solution for Qatar-5b, showing the velocity curve and observed velocities.

2.4 Follow-up photometry

Follow-up photometric observations for Qatar-3b and Qatar-4b were obtained with the 1.23m Zeiss Telescope at the Calar Alto Observatory (CAHA, Spain), using a Cousins-I filter and an exposure time of 60s per frame. For all observations, the telescope was defocused and data reduction was carried out using the DEFOT pipeline (Southworth 2009; Southworth et al 2014). Qatar-3b was observed on two occasions, on the 6th and the 11th of October 2015, while a half-transit of Qatar-4b was observed on the 27th of October 2015. Follow-up light curve for Qatar-5b was obtained using the KeplerCam on the 1.2m telescope at the Fred L. Whipple Observatory on Mount Hopkins, Arizona on the night of 10th November 2015. KeplerCam is equipped with a single 4K × 4K CCD covering an area of 23' × 23' on the sky. The observations were obtained through a SDSS-*i'* filter. Figures 5, 6 & 7 show the follow-up light curves together with the model fits described in Section 3.2.

To better determine the transiting systems ephemerides we fit the follow-up photometric curves with a transiting model following the prescription outlined in Pál et al. (2008). After the model fit, we estimate the T_C and calculate the best ephemerides. Because

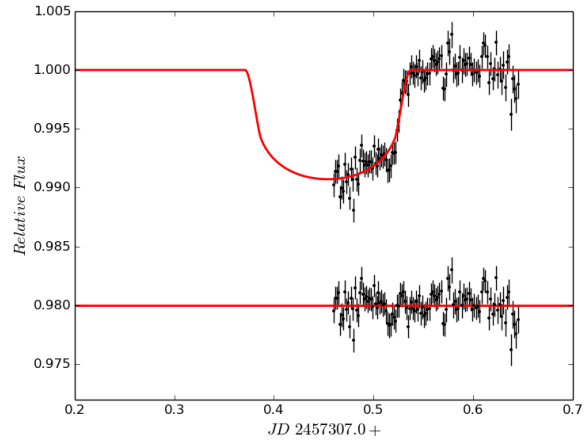
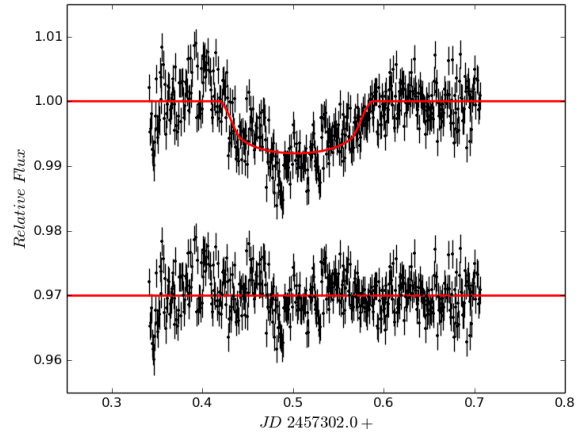


Figure 5. I-band follow-up light curves of Qatar-3b, obtained on 06/10/2015 (top panel) and 11/10/2015 (bottom panel) using the 1.23m Zeiss telescope at the Calar Alto observatory. The best-fit transit model overlaid in red (see text for details).

in some cases we could not observe a complete transit with high accuracy due to bad weather, some of our follow-up light curves have only partial coverage. In such cases we fixed the period to the value from the discovery light curve and left T_C as free parameter. For the current ephemerides, we used the T_C from the best model fit of the light curve.

$$T_{C,Q3b} = 2457302.453004 + E \cdot 2.5079204 \quad (1)$$

$$T_{C,Q4b} = 2457323.65441 + E \cdot 1.8053949 \quad (2)$$

and

$$T_{C,Q5b} = 2457336.758242 + E \cdot 2.8792319 \quad (3)$$

The errors of each value (eq. 1-2-3) are listed in Table 6.

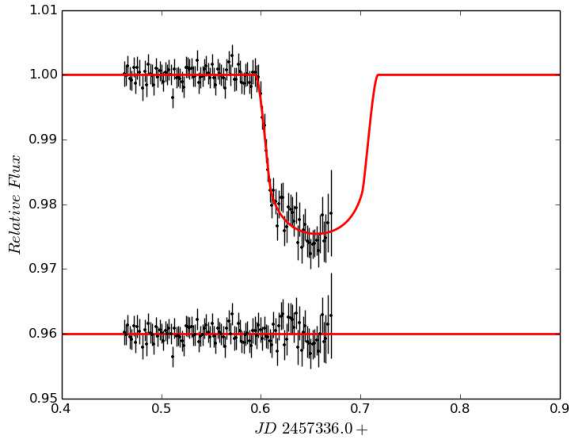


Figure 6. Same as Fig. 5, but for Qatar-4b, observed on 27/10/2015.

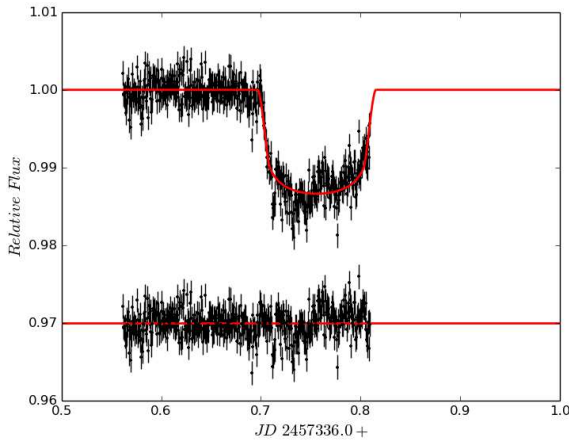


Figure 7. Same as Fig. 5, but for Qatar-5b, observed on 10/11/2015 with KeplerCam.

3 ANALYSIS AND RESULTS

3.1 Stellar Parameters

To improve the characterization of the three host stars, we analyzed the TRES spectra using the Stellar Parameter Classification (SPC) tool developed by Buchhave et al. (2012). In brief, the SPC cross correlates the observed spectrum with a library of synthetic spectra from Kurucz model atmospheres and finds the stellar parameters from a multi-dimensional surface fit to the peak correlation values. In addition, the stellar parameters — effective temperature (T_{eff}), metallicity ($[M/H]$), surface gravity ($\log g$), and projected rotational velocity $v \sin i$ — for the hosts were derived from the co-added spectra of each star through spectral modeling using the Spectroscopy Made Easy (SME) package (Valenti & Piskunov (1996)). The SPC results are reported in Table 1 and were used as initial guesses for the global fit of each system as described in the following section.

3.2 Planetary System Parameters

To determine the physical parameters of the three planetary systems we run a global solution of the available RV and transit photometric data using the EXOFAST package (Eastman et al. (2013)). As described by the authors, the EXOFAST performs a simultaneous fit of the RV and/or transit data for a single planet. In our case, for all the systems, we fixed the planetary orbital period to the value determined from the transits ephemerides and set the initial stellar parameters (T_{eff} , $\log g$, $[Fe/H]$) to the values determined from the spectroscopic analysis of the host stars.

The initial evaluation of the fits to the RV curves indicated they were all well described by circular orbits, i.e., $e = 0.0$. On one hand this is not surprising, as all three planets have short period orbits that are expected to have circularized. In addition, in the case of Qatar-4b, the RV curve has relatively few points and does not warrant detailed search for eccentric solution. In the case of Qatar-3b and Qatar-5b, we searched for eccentric solutions as well, but in both cases the results were essentially indistinguishable from $e = 0.0$ at the $\leq 2\sigma$ level. Consequently, in our global fits we kept the eccentricity fixed at $e = 0.0$. In addition, the period of each planet was kept fixed at the value determined by the transit ephemerides by in practice allowing it to vary only at the insignificant 10^{-5} d level.

Table 6 summarises the physical parameters of the planets¹.

4 CONCLUSIONS

Qatar-3b, Qatar-4b, and Qatar-5b are three new transiting hot Jupiters hosted by G0V, K1V, and G2V stars respectively. All three are short period planets ($P_{Q3b}=2.5079204$, $P_{Q4b}=1.8053949$, and $P_{Q5b}=2.8792319$ days) with masses and radii ($M_{Q3b}=4.31M_J$, $R_{Q3b}=1.096R_J$, $M_{Q4b}=5.85M_J$, $R_{Q4b}=1.552R_J$, $M_{Q5b}=4.32M_J$, $R_{Q5b}=1.107R_J$) in the expected regime for hot Jupiters, and densities ranging between 0.5- $2.5\rho_J$.

In Fig. 8, plot the transiting exoplanets with radii above $0.7R_J$. Red, green and blue dots are Qatar-3b, Qatar-4b, and Qatar-5b, respectively.

It should be noted that all three planets reside in the sparsely populated heavy-mass end ($M > 4M_J$) on the mass-radius diagram. In addition, the host of Qatar-5b is among the most metal-rich known parent stars.

ACKNOWLEDGEMENTS

This publication is supported by NPRP grant no. X-019-1-006 from the Qatar National Research Fund (a member of Qatar Foundation). The statements made herein are solely the responsibility of the authors.

D.F.E. is funded by the UK Science and Technology Facilities Council.

REFERENCES

- Alonso R. et al, 2004, ApJ, 613L, 153
 Alsubai K. et al. 2013, Acta Astron., 63, 465

¹ Assuming $R_{\odot}=696342.0$ km, $M_{\odot}=1.98855\times 10^{30}$ kg, $R_J = 69911.0$ km, $M_J=1.8986\times 10^{27}$ kg and 1 AU=149597870.7 km

Table 6. Median values and 68% confidence intervals. The host star age values has been calculated by Yonsei-Yale evolutionary tracks.

Parameter	Units	Qatar-3b	Qatar-4b	Qatar-5b
Stellar Parameters:				
M_*	Mass (M_\odot)	1.145 ± 0.064	0.954 ± 0.048	1.128 ± 0.056
R_*	Radius (R_\odot)	1.272 ± 0.14	1.115 ± 0.037	1.076 ± 0.051
L_*	Luminosity (L_\odot)	1.90 ± 0.46	0.829 ± 0.070	1.138 ± 0.12
ρ_*	Density (g/cm^3)	0.78 ± 0.20	0.972 ± 0.073	1.286 ± 0.15
$\log(g_*)$	Surface gravity (cgs)	4.286 ± 0.079	4.323 ± 0.023	4.427 ± 0.035
T_{eff}	Effective temperature (K)	6007 ± 52	5219 ± 50	5747 ± 49
[Fe/H]	Metallicity	-0.041 ± 0.081	0.166 ± 0.081	0.377 ± 0.080
age	Age [Gyr]	4.079 ± 1.34	12.90 ± 0.95	5.47 ± 4.40
Planetary Parameters:				
P	Period (days)	2.5079204 ± 0.0000099	1.8053949 ± 0.0000099	2.8792319 ± 0.0000099
a	Semi-major axis (AU)	0.03783 ± 0.00069	0.02861 ± 0.00048	0.04127 ± 0.00067
M_P	Mass (M_J)	4.31 ± 0.47	5.85 ± 0.47	4.32 ± 0.18
R_P	Radius (R_J)	1.096 ± 0.14	1.552 ± 0.057	1.107 ± 0.064
ρ_P	Density (g/cm^3)	4.0 ± 1.2	1.94 ± 0.22	3.95 ± 0.58
$\log(g_P)$	Surface gravity	3.942 ± 0.10	3.779 ± 0.041	3.940 ± 0.044
T_{eq}	Equilibrium Temperature (K)	1681 ± 84	1570 ± 26	1415 ± 31
Θ	Safronov Number	0.256 ± 0.035	0.226 ± 0.018	0.284 ± 0.016
$\langle F \rangle$	Incident flux ($10^9 \text{ erg s}^{-1} \text{ cm}^{-2}$)	1.81 ± 0.39	1.381 ± 0.094	0.910 ± 0.082
RV Parameters:				
K	RV semi-amplitude (m/s)	587 ± 58	1004 ± 71	568 ± 15
$M_P \sin i$	Minimum mass (M_J)	4.30 ± 0.47	5.85 ± 0.47	4.32 ± 0.18
M_P/M_*	Mass ratio	0.00360 ± 0.00036	0.00586 ± 0.00043	0.00366 ± 0.00011
γ	Systemic velocity (m/s)	542 ± 36	922 ± 60	416 ± 11
Primary Transit Parameters:				
T_C	Time of transit (BJD _{TDB})	$2457302.453004 \pm 0.00010$	$2457323.65441 \pm 0.00098$	$2457336.758242 \pm 0.000098$
R_P/R_*	Radius of planet in stellar radii	0.0888 ± 0.0018	0.1431 ± 0.0016	0.1061 ± 0.0013
a/R_*	Semi-major axis in stellar radii	6.39 ± 0.59	5.52 ± 0.14	8.27 ± 0.34
u_1	linear limb-darkening coeff	0.258 ± 0.047	0.408 ± 0.044	0.323 ± 0.043
u_2	quadratic limb-darkening coeff.	0.293 ± 0.050	0.214 ± 0.051	0.271 ± 0.048
i	Inclination (degrees)	86.8 ± 2.0	88.82 ± 1.2	88.74 ± 0.87
b	Impact Parameter	0.35 ± 0.22	0.114 ± 0.11	0.18 ± 0.16
δ	Transit depth	0.00789 ± 0.00032	0.02049 ± 0.00047	0.01126 ± 0.00028
T_{FWHM}	FWHM duration (days)	0.1173 ± 0.0017	0.1035 ± 0.0022	0.1089 ± 0.0012
τ	Ingress/egress duration (days)	0.0120 ± 0.0028	0.01526 ± 0.00069	0.01201 ± 0.0013
T_{14}	Total duration (days)	0.1296 ± 0.0034	0.1189 ± 0.0026	0.1212 ± 0.0015
P_T	A priori non-grazing transit prob	0.1426 ± 0.014	0.1552 ± 0.0041	0.1082 ± 0.0045
$P_{T,G}$	A priori transit prob	0.1703 ± 0.017	0.2070 ± 0.0055	0.1337 ± 0.0059
F_0	Baseline flux	1.00011 ± 0.00014	1.00003 ± 0.00016	0.99986 ± 0.00012
Secondary Eclipse Parameters:				
T_S	Time of eclipse (BJD _{TDB})	$2457303.706965 \pm 0.000100$	$2457324.55711 \pm 0.000970$	$2457338.197858 \pm 0.000098$

Barnes S., 2007, ApJ, 669, 1167

Bakos G., Noyes R. W., Kovács G., Stanek K. Z., Sasselov D. D.

& Domsa I., 2004, PASP, 116, 266

Batalha N. et al. 2013, ApJS, 204, 24

Bramich D. M. 2008, MNRAS, 386, L77

Buchhave L. A. et al., 2010, ApJ, 720, 1118

Buchhave L. A. et al., 2012, Nature, 486, 375

Eastman J., Gaudi B.S., & Agol E., 2013, PASP, 125, 83

Kovács G., Bakos G. and Noyes R., 2005, MNRAS, 356, 557

Kovács G., Zucker S. & Mazeh T., 2002, A&A, 391, 369

Pál A., 2008, MNRAS, 390, 281

Pollaco, D. L. et al, 2006, PASP, 118, 1407

Southworth J., 2009, MNRAS, 396, 1023

Southworth J. Hinse T., Burgdorf M. et al. 2014, MNRAS, 444, 776

Tamuz O., Mazeh T. and Zucker S., 2005, MNRAS, 356, 1466

Valenti J. A., & Piskunov, N., 1996, A&AS, 118, 595

Vidal-Madjar A., Lecavelier des Etangs, A. Désert J.-M. et al. 2008, ApJ, 676L, 57

This paper has been typeset from a \TeX / \LaTeX file prepared by the author.

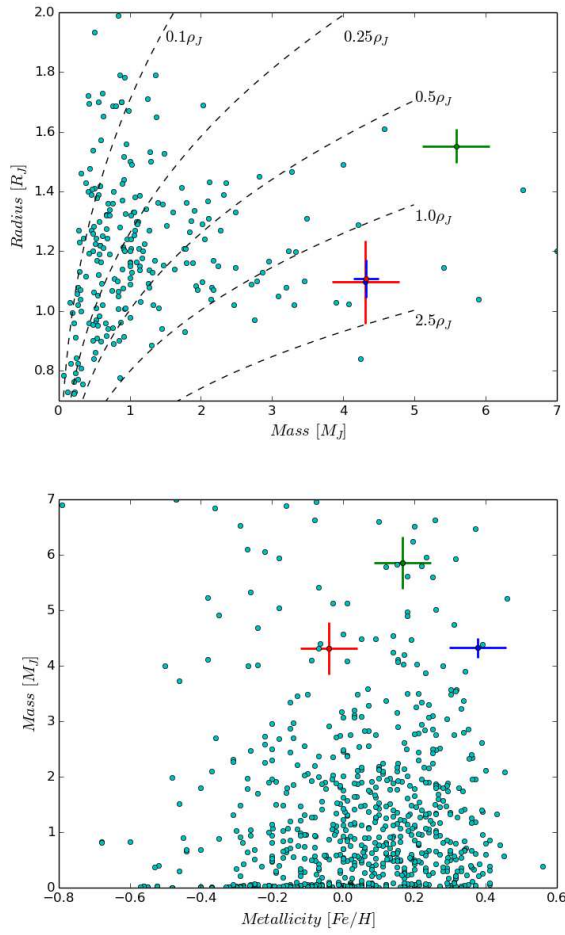


Figure 8. Radius-mass diagram of large exoplanets ($R_p \geq 0.7R_J$) (Top). Metallicity versus planetary mass (Bottom). Qatar-3b, Qatar-4b, and Qatar-5b are the red, blue and green dots, respectively.